Analyst

Accepted Manuscript

ROYAL SOCIETY OF CHEMISTRY

www.rsc.org/analyst

Manuscript for *Analyst* (Full paper)

Title:

Micro-thermography in millimeter-scale animals by orally-dosed fluorescent nanoparticle thermosensors

Satoshi Arai, ‡ [a] Ferdinandus, ‡ [b] Shinji Takeoka,[acd] Shin'ichi Ishiwata,[ade] Hirotaka Sato,*[b] and Madoka Suzuki*[ad]

a) Waseda Bioscience Research Institute in Singapore (WABIOS), SINGAPORE
b) School of Mechanical and Aerospace Engineering, Nanyang Technological University, SINGAPORE
c) Department of Life Science & Medical Bioscience, Graduate School of Advanced Science & Engineering, Waseda University, JAPAN
d) Organization for University Research Initiatives, Waseda University, JAPAN
e) Department of Physics, Faculty of Science and Engineering, Waseda University, JAPAN

*Corresponding authors

‡ These authors equally contributed to this work.

Abstract

We propose an instant micro-thermography using a fluorescent-nanoparticle thermosensor capable of reporting temperature as the fluorescence intensity ratio of temperature-sensitive dye to the reference. We demonstrate “temperature mapping” inside a fruit fly larva that was orally dosed with the nanoparticle thermosensors.

Introduction

Thermogenesis is a process to warm up the bodies in endothermic animals such as birds and mammals.[1] By sustaining the body temperature, organs and tissues can work at the optimal conditions in cold environments. In contrast, it is somewhat believed that the temperature in heterothermic animals is as the same as the surrounding. However, very recently, the endothermy in a certain type of fish (the opah), which has been considered as being cold-blooded, was discovered by Wegner’s group.[2] These fishes produce heat through flapping of wing-like pectoral fins under a deep and cold ocean to enhance the physiological performance during foraging. Their discovery implies what other species even not categorized in homothermic animals use endothermy to locally warm up some organs. Furthermore, some of heterothermic animals also possess thermoreceptor cells in the part of the body, sense the change in the external temperature and regulate their cellular functions.[3,4] Yet it is still unclear what the temperature distribution in their body is generated in response to the surrounding temperature and how the thermoreceptor cells localized in the bodies perceive the environmental temperature. To address these issues, it is straightforward to comprehend the temperature “inside animals” and its spatial distribution. The method for temperature mapping is expected to be one of the fundamental technologies.

Infrared thermography (IRT) has been a powerful means to meet these requirements. However, it is hardly applicable for wet biological samples where water molecules absorb the light at the region of infra-red wavelength. We can only speculate the internal temperature from the data as the surface temperature obtained as the black body irradiation. In addition, commercial infrared thermal cameras have limited spatial resolution (c.a. 10 μm) and thereby cannot be applied for cellular and tissue-level studies.[5] Fluorescent thermosensors are capable of reading out temperature as fluorescence signals such as fluorescence intensity, spectrum shift and lifetime. They have garnered attentions as a promising way to overcome the inherent limitations in IRT.[5,6] Up to date, various types of fluorescent thermosensors have been developed; e.g., organic small dyes,[7,8] inorganic particles,[9] nano-gel particles,[10] fluorescent proteins,[11] gold clusters[12] and dye-embedded polymeric particles.[13-15] These sensory materials are well-designed to be nanometer-sized with a view to high spatial resolution. More recently, some of them including ours achieved the visualization of temperature distribution in wet

biological samples such as living cells.[7-11,15] In particular, intensity-based (intensiometric) fluorescent thermosensors predominate in terms of temporal resolution down to microsecond orders,[16] whereas the other methods require a few seconds to minutes to make single images. Despite their promising feasibility, there have been scarce attempts to visualize temperature in living organisms of millimeter scale. A pioneering group only succeeded in visualizing temperature of C. *elegans* using green fluorescent proteins.[17] However, this methodology requires genetic engineering of the study animals, which interferes with its application to a wide variety of species.

In this paper, we propose a more accessible and easier-to-use method where polymeric particles as intensity-based fluorescent thermosensors are coupled with a simple oral dosing way for the delivery into the living organisms.[18] A brief account of a part of the present study was presented previously.[19] The benefit of an intensity-based thermometry includes the convenience that it requires only a conventional epi-fluorescence microscope widely used in modern biological laboratories. The problem shared among intensiometric measurements is that the fluorescence intensity is altered due to the movement of the animal, leading to the under or overestimation of the measurement. Thus, we developed a self-calibrating ratiometric fluorescent nanoparticle thermosensor (RNT) with both a temperature sensitive and a less-sensitive dye as an internal reference, which allows the correction of the displacement error. We further demonstrate the delivery of RNT to fruit fly larvae with orally dosing method, and the micro-thermography inside individual bodies.

Experimental section

General procedure. All organic solvents and chemical reagents were purchased from Sigma-Aldrich. Poly(vinylidenechloride-co-acrylonitrile) (PViCl-PAN) (Mw: 150000), poly(methyl methacrylate-co-methacrylic acid) (PMMA-MA) (Mn: 34000), poly(methyl methacrylate) (PMMA) (Mw: 94600), poly(styrene-co-methacrylic acid) (PS-MA) (Mw: 38000), polystyrene (Mw: 35000), polyvinylalcohol (PVA) (Mw:13000-23000) and tris(2-phenylpyridinato-C2,N)iridium(III) ($Ir(ppy)_3$) were purchased from Sigma-Aldrich. Eu-tris(dinaphthoylmethane)-bis-trioctylphosphine oxide (EuDT) was synthesized according to the previous literature (Shinsei Chemical Company Ltd).[20]

Preparation and characterization of RNTs. The polymeric particles were prepared according to previous reports.[13,15] Briefly, PS-MA (15 mg), EuDT (1.5 mg), and $Ir(ppy)_3$ (0.01 mg) were dissolved in 1 ml of tetrahydrofuran (THF) and then were added into 8 ml aqueous solution of PVA (160 mg). After being stirred at 1000 rpm for 1 hr at room temperature, the mixture was heated up and kept at 60 °C until THF evaporated completely. The resulting solution was

purified using a Sephadex PD column (GE Healthcare) to remove excess dyes. The hydrodynamic diameter and the surface charge of the resulting particles were characterized by Zetasizer ZSP (Malvern). The fluorescence was recorded using a fluorescence spectrophotometer (Hitachi F-2700).

Microscopy experiments. For florescence imaging experiments, an Olympus MVX10 Macro Zoom System Microscope with objective lenses MVPLAPO 1X, NA 0.25 and MVPLAPO 2XC, NA 0.5 were used for *in vivo* observation of PS-RNT in the larvae and for the observation of PS-RNT on the glass, respectively. An EM-CCD camera (iXon3 897; Andor Technology) was used to capture images. A FF01-405/10 excitation filter and a Di02-R442 dichroic mirror were used for excitation. A FF01-520/60 barrier filter was used to observe the fluorescence emission of $Ir(ppy)_3$ and a FF01-615/24 filter was used for EuDT. A Lumencor Spectra X light engine was used as the light source. The size of the observation field was 5.22×5.22 mm in 512×512 pixels for larvae and 0.84×0.84 mm in 512×512 pixels for substrate. Two-dimensional images were taken with an exposure time of 30 msec. For *in vivo* experiments, laboratory wild-type *Drosophila melanogaster* Canton Special (CS) strain larvae were chosen. They were fed with a mixture of fly food (Nutri-Fly BF, 50 μl) and the suspension of RNT (50 μl) for 2 days. After dosing, the larvae were washed with insect medium (Grace's Insect Medium, unsupplemented, 50 μl) to remove RNT adhered on the skin of the larvae. The larvae were placed on a glass slip and anaesthetized with cotton balls containing chloroform. To render the larvae exposed with the varying temperature, a microwarm plate (AS-One Kitazato) was used. During the microscopic experiments, two minutes waiting time was set to reach a stable temperature of the plate. A Ti400 Infrared camera (Fluke) with a 320×240 (76800) pixels was used for IR thermography. Invertebrates, including insects, are exempt from ethics approval for animal experimentation according to the National Advisory Committee for Laboratory Animal Research (NACLAR) guidelines.

Results and discussion

As a temperature sensitive dye, Eu-tris(dinaphthoylmethane)-bis(trioctylphosphine) oxide (EuDT) was synthesized according to the literature.[20] Previous fluorescent nanoparticle type thermosensors used Eu-thenolytrifluoroacetonate (EuTTA) and Eu-tris(dibenzoylmethane) -mono(phenanthroline).[13-15] However, both europium complexes suffer from low photostability and phototoxicity due to the excitation in the UV range. To improve this, we chose EuDT, which is known to be more photostable than EuTTA and excitable by a visible blue light around 400 nm with relatively lower phototoxicity.[20] As a temperature less-sensitive dye, tris(2-phenylpyridinato-C2,N) iridium ($Ir(ppy)_3$) was selected among hydrophobic dyes, which

can be excited with the same light source as that of EuDT. Because $Ir(ppy)_3$ is temperature less-sensitive than EuDT, we can engage the signal from $Ir(ppy)_3$ as an internal reference against EuDT in each nanoparticle in the ratiometric measurement. By using EuDT and $Ir(ppy)_3$, we prepared a ratiometric fluorescent thermosensor where both dyes were embedded into poly(styrene-co-methacrylic acid) (PS-MA) as a polymer matrix by a nanoprecipitation method, termed PS-RNT (Fig. 1a). The hydrodynamic diameter and zeta potential of PS-RNT were determined to be 122 ± 46 nm and –11.7 ± 0.6 mV, respectively (Fig. 1b). It is assumed that PVA as a charge-free neutral polymer formed a hydrophilic outer layer of the nanoparticle, while the carboxyl group of PS-MA oriented to the surrounding water provide a slightly negative charge. These factors should contribute to stabilize the stable suspension. The temperature sensitivity of PS-RNT was evaluated using the fluorescence spectrophotometer. The ratio value (I_{615}/I_{506}) calculated from the fluorescence of EuDT and $Ir(ppy)_3$ was plotted against varied temperature and the slope obtained from its calibration curve is defined as the temperature sensitivity (%/°C). The PS-RNT exhibited a higher temperature sensitivity, –0.039/°C (–4.0 %/°C relative to 36 °C), than previous ones about –2 - –3 %/°C (Fig. 1c, d).[15,21] Also, PS-RNT showed the reversible fluorescence response in accordance with the change in temperature (Fig. S1, Supporting Information).

Regarding a polymer matrix to form the particle, we tested several polymers including PS-MA; poly(methylmethacrylate) (PMMA), poly(methylmethacrylate-co-methacrylic acid) (PMMA-MA), polystyrene (PS), and poly(vinylidene chloride-co-acrylonitrile) (PViCl-PAN). The PMMA and PS resulted in precipitation during the preparation process, whereas others successfully formed stable suspensions of particles. The sensitivity differed among polymers but all of them displayed the decrease in fluorescence with the increase in temperature (see Table S1 and S2, Supporting Information). The temperature sensitivity of an europium complex follows the principle where the energy transfer from ligands to the central Eu^{3+} ion via the non-radiative process is preferred as temperature increases.[22] The different polymer matrix may interact with dinaphthoylmethane ligand of EuDT differently affecting the sensitivity although the mechanism is still unclear. In terms of the sensitivity, PS-MA was finalized as a matrix to prepare the nanoparticle.

We next validated PS-RNT by using a fluorescence stereomicroscopy. The buffer solution containing PS-RNT was casted on the glass substrate. Single dots were observed in both $Ir(ppy)_3$ and EuDT channels as shown in Fig. 2a. As the substrate was heated up from 26 to 44 °C, the change in fluorescence intensity in EuDT and $Ir(ppy)_3$ channels were analyzed in each region of interest (ROI) set on each dot, and the ratio value (EuDT/$Ir(ppy)_3$) was plotted against the substrate temperature (Fig. 2b, as representatives). The average of ratio values was plotted with standard deviation (SD) as shown in Fig. 2c. The sensitivity obtained from the

slope was determined to be –0.021/°C, which is less sensitive than that in the cuvette experiments (–0.040/°C). This is because the fluorescence intensity measured can vary among the experimental setups. All the excitation light intensity and band width, the sensor gain, and the band width for emission light will affect the fluorescence intensity in each channel. These results give the caution that the calibration should be performed in each setup.[15] In the re-cooling process from 44 to 26 °C, the response to the change in temperature was almost identical to the process in heating, indicating that PS-RNT responds to the change in temperature reversibly, and, as expected, the photobleaching is negligible (Fig. S2, Supporting Information). The temperature resolution in this thermometry, namely the accuracy, was defined as δT at each temperature [$\delta T(T)$], where the SD of fluorescence ratio was divided by the overall temperature sensitivity.[10,23] The δT was within 0.4 to 0.8 °C at T between 26 and 44 °C. The single dot can be attributed to an aggregate of single particles because the particles are likely to aggregate each other during the evaporating process of the suspension on the glass. Regardless of the size of aggregations, the SD of fluorescence ratio was notably narrow; the accuracy was comparable with previous fluorescence thermometry.[15,23] This is another virtue of the ratiometric thermometer that the ratio value is independent of the concentration of dyes.

We further demonstrated PS-RNT in temperature mapping inside a fruit fly larva. A fruit fly has been widely used as a model organism for various biological studies such as physiology and life history theory. Its larva is also compatible with fluorescence imaging experiments because of its relatively transparent body and thereby was chosen here as a model for micro-thermography. Firstly, we optimized the mixed ratio of the fly food to the PS-RNT suspension, which rarely affected the survival rate of larvae through oral dosing within the range we tested (Table S3, Supporting Information). The larvae were orally dosed with the optimal fly food containing PS-RNTs, and they were cultured for 2 days until the time of observation. The fluorescence of PS-RNTs was observed in both channels primarily at the location of guts. Insects absorb digested foods at the mid- and hindguts.[24] Substantial amount of PS-RNTs appeared to remain in the guts without being digested during this 2-day-incubation. The background signal due to the autofluorescence was recognized in $Ir(ppy)_3$ channel, whereas it was substantially low in EuDT channel (Fig. 3a). Then, the larvae were subjected to the change in external temperature on a glass substrate. The intensity in each camera pixel in EuDT channel was divided by the value of the corresponding pixel in $Ir(ppy)_3$ channel. The resulting images at each external temperature are shown as ratio images in Fig. 3b. The averages of ratio values at different ROIs were plotted against the external temperature. As a result, the similar slope with that of the substrate was obtained (Fig. 3d). The δT was determined to be within 1.0 to 1.7 °C, which was bigger than that on the substrate. The reversibility of PS-RNTs in the larva was also confirmed (Fig. S3, Supporting Information). The signal from non-dosed larvae

showed the constant level of autofluorescence at the temperature between 24 and 42 °C (Fig. S4, Supporting Information). The chemical environment in larva body is considered to be distinct from the glass substrate. The consistent results from these two extremely different conditions support the specificity of dye-embedded polymeric nanoparticles to the temperature. As we and others have discussed previously for single cell conditions, the temperature specificity is also considered as prerequisite property for *in vivo* uses.[25-27]

One of the key issues is the accuracy of this thermometry, δT. The δT was larger inside the larva than that on the substrate even by using the same microscopy setup. This result may suggest the temperature distribution inside the larva. This is one of the positive examples in our thermometry proposed in this paper because it is difficult to visualize these distributions at millimeter scale by using commercial IRT as shown in Fig. 3c. However, we cannot simply attribute the larger δT to the internal temperature distribution. Although the autofluorescence was independent of the external temperature, it cannot be ignored in the low fluorescence region in $Ir(ppy)_3$, leading to the over- or underestimation of the ratio values. These problems need to be solved in future, for example, by using near-infrared dyes. This improvement will further expand the application towards other species including less-transparent samples.

Conclusions

In this paper, we fabricated a self-calibrated fluorescent-nanoparticle thermosensor, PS-RNT. By using this PS-RNT with orally dosing method, we achieved the temperature mapping in a fruit fly larva. The preparation method of PS-RNT is simple, providing the advantage in *in vivo* applications where large amount of the fluorescent thermosensors are required. The simplicity using a common fluorescence microscope and an easy-handling fluorescent thermometer as presented here will be indispensable properties towards the standardization of micro-thermography in the wide-ranging fields in which not only material scientists are employed, but also biologists as well as zoologists work together. In future, it will be required beyond the oral-dosing way to deliver the thermosensors into specific tissues, or even to cells. Recent reports stress the importance of the distance between the thermometer and the target for the accurate temperature measurement.[8,11,15,26] Therefore, targeting ability will possibly provide more precise thermometry in the living organisms.

Acknowledgments

The authors thank Dr. Stephen Cohen (A*STAR) for the gift of fruit flies. This research was partially supported by Nanyang Assistant Professorship (NAP) (to H.S.), A*STAR (Agency for Science, Technology and Research, Singapore)-JST (The Japan Science and Technology Agency) joint grant (to H.S. and S.I), and Japan Society for the Promotion of Science (JSPS)

KAKENHI Grant Numbers 15K05251 and 26107717 (to M.S.). The authors thank Shinsei Chemical Company Ltd. for synthetic supports (the dye, EuDT).

References

1 B. B. Lowell and B. M. Spiegelman, *Nature*, 2000, **404**, 652–660.

2 N. C. Wegner, O. E. Snodgrass, H. Dewar and J. R. Hyde, *Science*, 2015, **348**, 786–789.

3 K.-I. Takeuchi, Y. Nakano, U. Kato, M. Kaneda, M. Aizu, W. Awano, S. Yonemura, S. Kiyonaka, Y. Mori, D. Yamamoto and M. Umeda, *Science*, 2009, **323**, 1740–1743.

4 W. W. Liu, O. Mazor and R. I. Wilson, *Nature*, 2015, **519**, 353–357.

5 C. D. S. Brites, P. P. Lima, N. J. O. Silva, A. Millán, V. S. Amaral, F. Palacio and L. D. Carlos, *Nanoscale*, 2012, **4**, 4799–4829.

6 X.-D. Wang, O. S. Wolfbeis and R. J. Meier, *Chem. Soc. Rev.*, 2013, **42**, 7834–7869.

7 O. Zohar, M. Ikeda, H. Shinagawa, H. Inoue, H. Nakamura, D. Elbaum, D. L. Alkon and T. Yoshioka, *Biophys. J.*, 1998, **74**, 82–89.

8 S. Arai, S.-C. Lee, D. Zhai, M. Suzuki and Y. T. Chang, *Sci. Rep.*, 2014, **4**, 6701.

9 J. Yang, H. Yang and L. Lin, *ACS Nano*, 2011, **5**, 5067–5071.

10 K. Okabe, N. Inada, C. Gota, Y. Harada, T. Funatsu and S. Uchiyama, *Nat. Commun.*, 2012, **3**, 705.

11 S. Kiyonaka, T. Kajimoto, R. Sakaguchi, D. Shinmi, M. Omatsu-Kanbe, H. Matsuura, H. Imamura, T. Yoshizaki, I. Hamachi, T. Morii and Y. Mori, *Nat. Methods*, 2013, **10**, 1232–1238.

12 L. Shang, F. Stockmar, N. Azadfar and G. U. Nienhaus, *Angew. Chem. Int. Ed.*, 2013, **52**, 1–5.

13 K. Oyama, M. Takabayashi, Y. Takei, S. Arai, S. Takeoka, S. Ishiwata and M. Suzuki, *Lab Chip*, 2012, **12**, 1591–1593.

14 X. Wang, X. Song, C. He, C. J. Yang, G. Chen and X. Chen, *Anal. Chem.*, 2011, **83**, 2434–2437.

15 Y. Takei, S. Arai, A. Murata, M. Takabayashi, K. Oyama, S. Ishiwata, S. Takeoka and M. Suzuki, *ACS Nano*, 2014, **8**, 198–206.

16 P. A. Quinto-Su, M. Suzuki and C.-D. Ohl, *Sci. Rep.*, 2014, **4**, 5445.

17 J. S. Donner, S. A. Thompson, C. Alonso-Ortega, J. Morales, L. G. Rico, S. I. C. O. Santos and R. Quidant, *ACS Nano*, 2013, **7**, 8666–8672.

18 Ferdinandus, S. Arai, S. Ishiwata, M. Suzuki and H. Sato, *PLoS One*, 2015, **10**, e0116655.

19 Ferdinandus, S. Arai, S. Ishiwata, M. Suzuki and H. Sato, *Solid-State Sensors, Actuators and Microsystems, 2015 Transducers XXVIII: The 18th International Conference on*, 2015, 2228–2231.

20 M. D. McGehee, T. Bergstedt, C. Zhang, a. P. Saab, M. B. O'Regan, G. C. Bazan, V. I. Srdanov and a. J. Heeger, *Adv. Mater.*, 1999, **11**, 1349–1354.

21 K. Oyama, M. Takabayashi, Y. Takei, S. Arai, S. Takeoka, S. Ishiwata and M. Suzuki, *Lab Chip*, 2012, **12**, 1591–1593.

22 B. B. J. Basu and N. Vasantharajan, *J. Lumin.*, 2008, **128**, 1701–1708.

23 C. Gota, K. Okabe, T. Funatsu, Y. Harada and S. Uchiyama, *J. Am. Chem. Soc.*, 2009, **131**, 2766–2767.

24 R. F. Chapman, The insects: structure and function. New York: Cambridge university press., 1998, 770.

25 G. Baffou, H. Rigneault, D. Marguet and L. Jullien, *Nat. Methods*, 2014, **11**, 899–901.

26 M. Suzuki, V. Zeeb, S. Arai, K. Oyama, and S. Ishiwata, *Nat. Methods* (*in press*).

27 C. Paviolo, A. H. A. Clayton, S. L. McArthur, P. R. Stoddart, *J. Microsc.*, 2013, **250**, 179–188.

Figure 1. Characterization of PS-RNT. a) Schematic illustration of PS-RNT. EuDT as a temperature sensitive dye (red closed circle) and $Ir(ppy)_3$ as an internal reference (blue closed square) are embedded into single PS-MA polymeric nanoparticle whose surface is stabilized with the hydrophilic layer (light blue shell) provided by PVA. b) Size distribution of PS-RNT in the PBS buffer solution measured by dynamics light scattering, 122 ± 46 nm. c) Fluorescence spectrum of PS-RNT at varied temperature. The excitation wavelength was 390 nm and the emission was recorded from 490 to 650 nm. d) To support the graph (c), the fluorescence ratio (I_{615}/I_{506}) was plotted versus varied temperature. Error bars, SD (n = 3).

Figure 2. Fluorescence microscopic observation of PS-RNT on the glass substrate. a) Bright dots were observed under a fluorescence stereo microscope. The upper panel is the fluorescence image in $Ir(ppy)_3$ channel and the lower in EuDT channel. Scale bars, 100 μm. b) The average values of fluorescence intensity at the region of interest (ROI) covering a single dot was plotted for ROI1 and ROI2 against varying temperature of the substrate in both $Ir(ppy)_3$ (blue open circle) and EuDT (red open circle) channels. The fluorescence ratio (EuDT/$Ir(ppy)_3$) calculated from these values was plotted as black closed circle. c) The average of the ratio of different ROIs (18 ROIs) was calculated at each temperature. The change of the ratio in response to the heating (from 26 to 44 °C, magenta closed circles) and cooling (from 44 to 26 °C, cyan closed circles) was plotted with SD. The calibration slope obtained from heating is –0.021/°C ($y = -0.021x + 1.5$, $R_2 = 0.97$). The temperature resolution was defined at each temperature as δT, where the SD is divided by the temperature sensitivity (0.021/°C).

Figure 3. Fluorescence micro-thermography in a fruit fly larva. a) The fluorescence images of a fruit fly larva obtained under a fluorescence stereo microscope. The larva was orally dosed with PS-RNT. Left, $Ir(ppy)_3$ channel. Right, EuDT channel. Scale bar, 500 μm. The larva at the very left is a control without dosing PS-RNT (Ctrl). b) Micro-thermography of larvae using fluorescence ratio (EuDT/$Ir(ppy)_3$). Scale bar, 500 μm. c) Left, a bright field image of two larvae. Right, an IRT image in the same field of view as in *left*. d) The average of the ratio of different ROIs (15 ROIs) was plotted at each temperature with SD. The calibration slope obtained from heating is –0.024/°C ($y = -0.024x + 1.7$, $R^2 = 0.99$). The temperature resolution was defined at each temperature as δT where the SD is divided by the temperature sensitivity (0.024/°C).

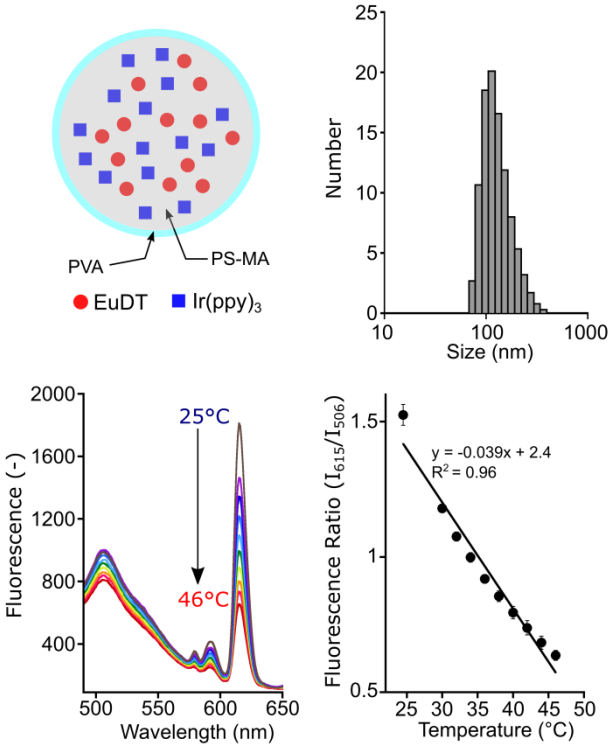

Figure 1. S. Arai et al

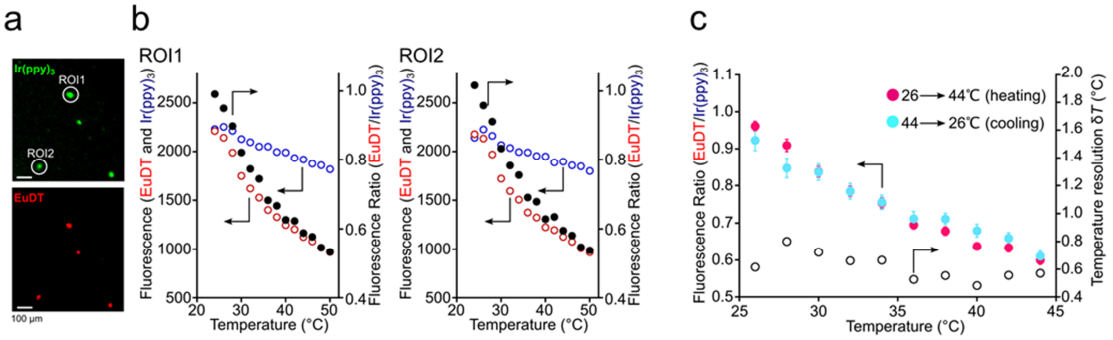

Figure 2. S. Arai et al

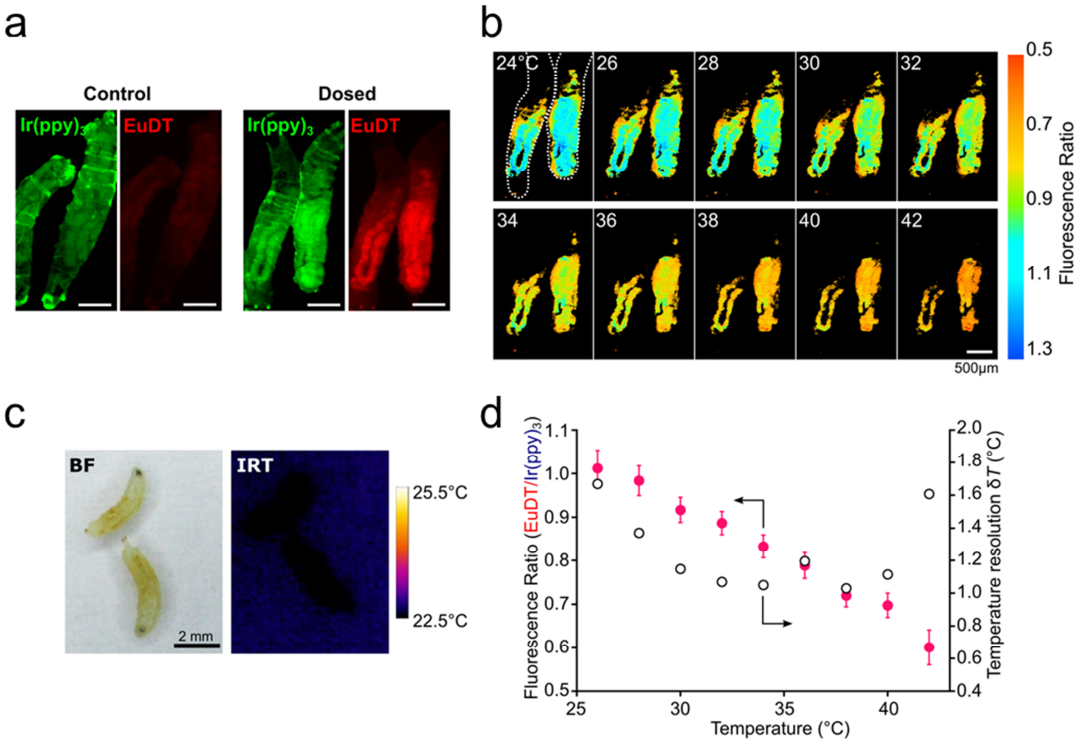

Figure 3. S. Arai et al

Table of contents

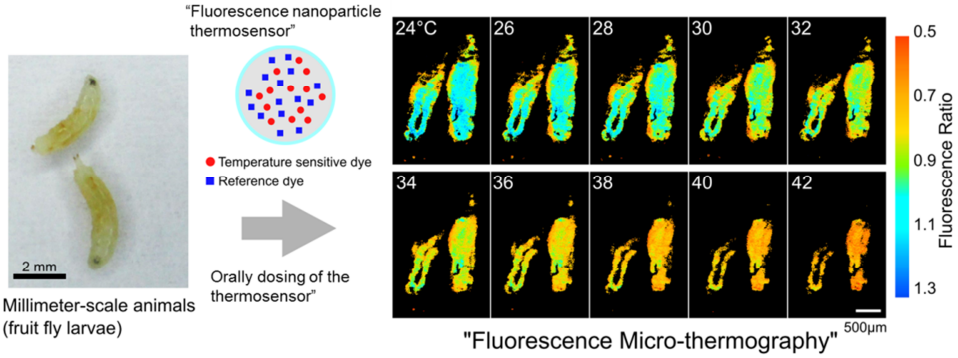

Temperature mapping inside a fruit fly larva that was orally dosed with the fluorescent nanoparticle thermosensors